Pergamon

Vision Res., Vol. 36, No. 14, pp. 2047–2060, 1996

0042-6989(95)00314-2

Printed in Great Britain
0042-6989/96 $15.00 + 0.00

Linear and Nonlinear Contributions to Step Responses in Cat Retinal Ganglion Cells

J. F. COX,*† M. H. ROWE*‡

Received 20 June 1995; in revised form 30 October 1995

We measured excitatory and inhibitory step responses of cat retinal ganglion cells to square wave contrast reversal of stationary sinusoidal gratings. In most Y-cells the initial increase in firing rate (early peak) of the excitatory responses was followed by a distinct second increase in firing rate (late peak). Analysis of the spatial frequency and spatial phase dependence of the two peaks indicated that the early peak appears to be produced by the spatially linear center mechanism, while the late peak appears to be produced by the rectifying subunits described by Hochstein and Shapley (1976) ***Journal of Physiology, London, 262,*** **237–264, 265–284.**

These results indicate that the presence of two peaks in ganglion cell step responses is the result of two excitatory inputs with different time courses, and that inhibitory inputs are not required to explain the appearance of these responses. Copyright © 1996. Published by Elsevier Science Ltd.

Retinal ganglion cells Y-cells Step responses Linear systems Rectification

INTRODUCTION

Responses to stimuli presented as prolonged square pulses or with low frequency square wave temporal modulation, which we will refer to herein as step responses, have long been used in the study of retinal ganglion cell physiology. For example, since the earliest descriptions of X- and Y-cells in the cat retina (Enroth-Cugell & Robson, 1966), it has been noted that under light adapted conditions the time courses of Y-cell step responses were more transient that those of X-cells, and this observation has been confirmed many times (e.g. Cleland *et al.*, 1971; Ikeda & Wright, 1972; Enroth-Cugell & Shapley, 1973; Hammond, 1975; Jakiela *et al.*, 1976). Another reported difference between X- and Y-cells is that the step responses of Y-cells often contain a second rise in firing rate superimposed on the falling phase of the initial transient response (Saito *et al.*, 1971). Similar two-peaked responses had previously been observed in some ganglion cells by Winters and Walters (1970), although these authors did not emphasize differences between cell classes. Saito *et al.* (1971) suggested that the discontinuity between the first and second peaks in Y-cell step responses was due to timing differences between excitatory and inhibitory mechanisms, and other authors imposed similar interpretations. For example, DeMonasterio (1978) observed two distinct peaks in the step responses of Y-like ganglion cells in primate retina, and suggested that the dip between them represented a transient inhibition, arising in amacrine cells, and presumably interrupting a single excitatory input. Richter and Ullman (1982) subsequently incorporated such amacrine inhibition into a formal model of the temporal behavior of primate ganglion cells.

However, there is no direct evidence to support the transient inhibition hypothesis, and other possible explanations have not been examined. In this study, we wanted to characterize the step responses of cat retinal ganglion cells within the framework of established receptive field mechanisms. Specifically, we tested the hypothesis that the two peaks in Y-cell step responses are produced by differences in timing between two excitatory inputs: one from the spatially linear center mechanism and one from the rectifying subunit mechanisms that have been described in Y-cell receptive fields (Hochstein & Shapley, 1976a,b; Victor, 1988). Our results clearly indicate that this is the case; the initial peak is generated primarily by the center mechanism, while the second peak is generated by rectifying subunits. These two excitatory inputs appear to be combined in an approximately additive manner to produce the overall shape of the step response, and thus there is no need to invoke any form of transient inhibition to explain the appearance of these responses. Some of these results have been previously presented in Abstract form (Cox & Rowe, 1993).

*Neurobiology Program, Department of Biological Sciences, Ohio University, Athens OH 45701, U.S.A.

†Present Address: Department of Ophthalmology, Children's Hospital, 700 Children's Drive, Columbus OH 43205-2696, U.S.A.

‡To whom all correspondence should be addressed [*Email* rowe@mail.oucom.ohiou.edu].

METHODS

General preparation

Data were collected from 14 adult cats. Anesthesia was induced with 4% halothane, administered in a 70:30 mixture of nitrous oxide (N_2O) and oxygen (O_2). Subsequently, an i.v. catheter was inserted into the radial vein, nembutal (20 mg/ml) was administered i.v. to maintain a surgical level of anesthesia, and the gaseous anesthesia was discontinued. Injections of 100 μg dexamethasone, 1 mg atropine and 1 ml of a veterinary antibiotic–antimycotic mixture were given intramuscularly into the gastrocnemius/soleus. A tracheotomy and right unilateral sympathectomy were performed, and the cat was then mounted in a stereotaxic head holder that did not obstruct the visual fields. Then, the skull was exposed with a midline scalp incision and two small holes were drilled directly above the optic chiasm (anterior 12, lateral ± 2 mm), for placement of stimulating electrodes in the optic chiasm (OX). Two smaller holes were made over the visual cortical region to allow placement of stainless steel screws from which the EEG was monitored. To diminish circulatory and respiratory pulsations during the recording session, a cisternal drainage was performed, and the animal's body was suspended with a spinal clamp attached to a thoracic vertebra.

All recordings were made from the right eye. Phenylephrine drops (10%, Neosynephrine) were applied topically to retract the nictitating membrane, and atropine (1%) drops were applied to dilate the pupils. Artificial pupils were not used. The eye was fitted with a zero-power plastic contact lens that was wetted with a commercial lens-soaking solution. The eye was mounted on a metal ring secured to the stereotaxic apparatus via conjunctiva attachment, and a small hole was made in the sclera, *c.* 6 mm posterior to the limbus, to allow insertion of a metal guide tube. This tube was mounted in a ball and socket joint which allowed three-dimensional rotation of the guide tube around the point of entry into the eye.

Following initial surgery, the cat was paralyzed with a 40 mg loading dose of flaxedil and paralysis was maintained with a continuous i.v. infusion of (5–8 mg/kg/hr) flaxedil in 0.9% saline. The cat was artificially ventilated, and expired CO_2 levels were maintained between 3.7 and 4.5%. Subscapular temperature was maintained at 37°C via a homeostatically regulated heating blanket. Anesthesia was maintained by i.v. infusion of nembutal (1–1.5 mg/kg/hr), and the depth of anesthesia was assessed by monitoring EEG and EKG signals. Supplemental doses of i.v. nembutal were given whenever either of these showed evidence that anesthesia was becoming lighter.

Retinal recording. The cat was positioned so that it faced a tangent screen located directly in front of it at a distance of 171 cm. During recording, receptive fields were hand plotted on this screen using small flashing spots of light. A beam-splitter was also positioned in front of the animal which allowed the image of a CRT screen (Tektronix 608) to be reflected into the cat's eye along an optical path that was 57 cm long. The orientation of the beam-splitter could be adjusted as needed to center receptive fields on the CRT screen. Spectacle lenses were used to focus the eye on the CRT screen employing the tapetal reflection method of Pettigrew *et al.* (1979). Tapetal reflection was also used to plot the locations of the optic disc and area centralis on the tangent screen.

Glass micropipettes filled with 1 M NaCl and having impedances between 10 and 20 MΩ were used to isolate the spike activity of single retinal ganglion cells. Spikes generated by ganglion cell somas could easily be distinguished from those generated by axons on the basis of their waveform. The electrodes were inserted through the guide tube and advanced towards the retina by means of an electronically controlled stepper motor (nanostepper, WPI) which was supported by an apparatus which provided precise three-dimensional rotation of the entire electrode-stepper motor assembly about the point of entry into the eye. Antidromic spikes were elicited by passing 50–100 μsec pulses of 5–50 V amplitude through the OX electrodes. The spikes were displayed on a digital oscilloscope and latencies were measured to the nearest 0.1 msec. Optic chiasm stimulation routinely elicited t_1 and t_2 field potentials which are widely believed to reflect activity in the axons of Y- and X-cells, respectively (Rowe & Stone, 1976). Thus, we were able to determine the optic chiasm latencies of local Y- and X-cell populations on virtually every electrode penetration, making optic chiasm latency the most reliable parameter for identification of individual cells as Y or X. Receptive field size, responses to stationary and moving stimuli, and linearity of spatial summation were also used for identification. Cells with optic chiasm latencies in the t_2 range, small receptive fields, tonic responses to stationary flashing spots, poor responsiveness to fast moving targets, and exhibiting a clear null position for stationary, counterphased sinusoidal gratings were identified as X. Cells with optic chiasm latencies in the t_1 range, large receptive fields, good responsiveness to fast moving targets, and exhibiting spatial phase independent frequency doubled responses to stationary, counterphased sinusoidal gratings were identified as Y.

Visual stimulation. All visual stimuli were generated by a Picasso Image Generator and presented on the CRT screen. The mean luminance of this screen, viewed through the beam-splitter, was 3 cd/m^2. Step responses were generated with stationary sine wave gratings whose contrast was periodically reversed in a square wave pattern. Gratings positioned in odd symmetry with respect to the center of the receptive field were designated as having a spatial phase of 0, and all other phase positions were specified in units of degrees relative to the 0 phase position. Peristimulus histograms were collected with a binwidth of either 1.0 or 1.953 msec, and responses were typically averaged over 20–50 stimulus cycles. These histograms were typically filtered digitally with a gaussian filter whose standard deviation was generally 9–13 msec, prior to further analysis. Supple-

mental analyses, e.g. to determine contrast sensitivity profiles, were performed using drifting sine wave gratings of fixed contrast, or stationary gratings whose contrast was modulated according to a sinusoidal time course. In these cases, histograms were subjected to a Discrete Fourier transform, and the mean-to-peak amplitudes (in units of spikes · sec^{1}) of the fundamental (F1) and second harmonic (F2) components in the response were measured, along with amplitude of the DC or average firing rate.

Procedure

Spatial tuning. For each cell encountered, we first assessed its spatial tuning characteristics. Generally, for each of a series of spatial frequencies, the contrast of a drifting grating was adjusted so that the cell's response was just above threshold, as judged by listening over the audio monitor. The amplitude of the F1 component was then measured, and responsivity, in units of impulses · sec^{1} · $contrast^{1}$, was calculated by dividing response amplitude by stimulus contrast (Enroth-Cugell *et al.*, 1983). Measured responsivity values were fitted with a difference of gaussian (DOG) function, $S(\nu) = K_c \pi r_c^2 e^{-(\pi r_c \nu)^2} - K_s \pi r_s^2 e^{-(\pi r_s \nu)^2}$, where S is the overall responsivity, ν is spatial frequency, K_c and K_s are the peak responsivities, respectively, of the center and surround mechanisms, and r_c and r_s are the respective radii, in degrees, of the gaussian center and surround profiles at the point where their responsivities have declined to $1/e$ of their peak values (Linsenmeier *et al.*, 1982). It should be emphasized that throughout this paper, the term *surround* is used only to refer to the linear surround mechanism of the receptive field, and does not include any other mechanisms that might reside in the region outside the receptive field center. Fits were performed off-line using an iterative curve-fitting program, based on the Nelder–Mead algorithm (Nelder & Mead, 1965). Initial values for the curve-fitting program were obtained from a separate program. Center parameters (r_c, K_c) were first estimated by fitting a single gaussian profile to measured responses at or above the peak spatial frequency. After subtracting this fitted profile from the measured responses at all spatial frequencies tested, surround parameters (r_s, K_s) were estimated by fitting a second gaussian profile to the remainder. In a few cases, the optimal spatial frequency was selected qualitatively by estimating thresholds in terms of audio criteria.

Step responses. Step responses were then elicited using stationary gratings, whose contrast was periodically reversed according to a 0.5 Hz square wave time course. Since contrast reversal was used, the absolute value of contrast was constant throughout the stimulus cycle, thus minimizing the influence of the contrast gain control mechanism on the measured step responses. In some cases responses were obtained at a number of spatial frequencies at or above the peak of the spatial tuning curve of the cell. For each spatial frequency tested, step responses were first measured at 0 spatial phase, defined as the position of odd symmetry with respect to the receptive field. This was established by finding a spatial phase at which the F1 response was absent. The spatial phase of the grating was then shifted by 90 deg, and step responses measured at that position. In most cases, the phase was then rechecked by returning the grating to the 0 phase position and confirming that the F1 response was still absent. For a subset of cells, step responses were also obtained at spatial phases of 22.5, 45 and 67.5 deg. (It should perhaps be noted that, since the negative step response at any spatial phase is equivalent to the positive step response at that phase ± 180 deg, these measurements over the range of 0–90 deg are equivalent to measuring positive step responses over a full half-cycle of the grating. We felt, however, that the convention of positive and negative responses at a single spatial phase better suited the logic of this experiment.) In most of these cases, measurements were made at a single spatial frequency at or above the peak of the cell's spatial tuning curve. In some cases step responses were also obtained at more than one contrast, within the range of 15–45%.

Positive step response profiles were subjected to two forms of quantitative analysis designed to estimate the separate contributions of phase-dependent and phase-invariant response mechanisms to the overall response. One method is referred to as the "decomposition analysis" and the other as the "subtraction analysis". In the decomposition analysis, we assumed that for each of the four stimulus phases used the overall response at any point in time consisted of the algebraic sum of a phase-invariant component and a phase-dependent component. It was further assumed that the phase dependence was sinusoidal. These assumptions are embodied in the following equation:

$$\text{Response(phase)} = A + B \sin(\text{phase}) + \text{error}$$

where A is the amplitude of the phase invariant component, and B is the amplitude of the phase dependent component. For each point in time we wrote four such equations, one for each of the four response profiles, plugged values from the 22.5, 45.0, 67.5, and 90 deg response profiles into the left half of the appropriate equation, and then solved for A and B iteratively using the Nelder–Mead algorithm (Nelder & Mead, 1965), so that the sum of the squared error terms was minimized.

The resulting array of B values, scaled by the sine of the spatial phase, depicted the estimated time course of the phase-dependent response component. Similarly, the array of A values showed the estimated time course of the phase-invariant response component which, with this procedure, also included the DC or maintained firing rate of the cell. In order to facilitate comparisons between measured and derived profiles, the DC component has been removed in some illustrations. Since the response at zero spatial phase was an empirical measure of the phase-invariant component, a comparison between the array of A values and the measured response profile at 0 deg served as a check on the validity of the decomposition analysis. These two profiles were compared statistically

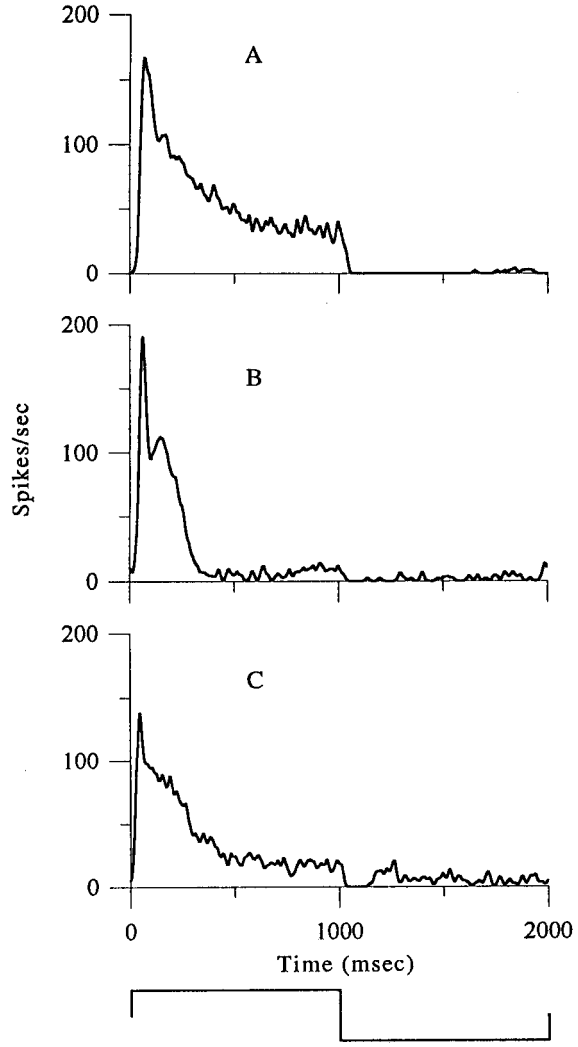

FIGURE 1. Positive and negative step responses of an on center X-cell (A) and two Y-cells (B,C). In each case, the two responses are shown as a single histogram, arbitrarily arranged so that the positive response occurs first. The stimuli used were sinusoidal gratings positioned in even symmetry with respect to the receptive field center. Spatial frequencies were 0.3 c/deg (top), 0.1 c/deg (middle), and 0.2 c/deg (bottom). The time course of the stimulus waveform is shown at the bottom. The contrast used was 37% in the top and middle histograms, and 25% in the bottom histogram.

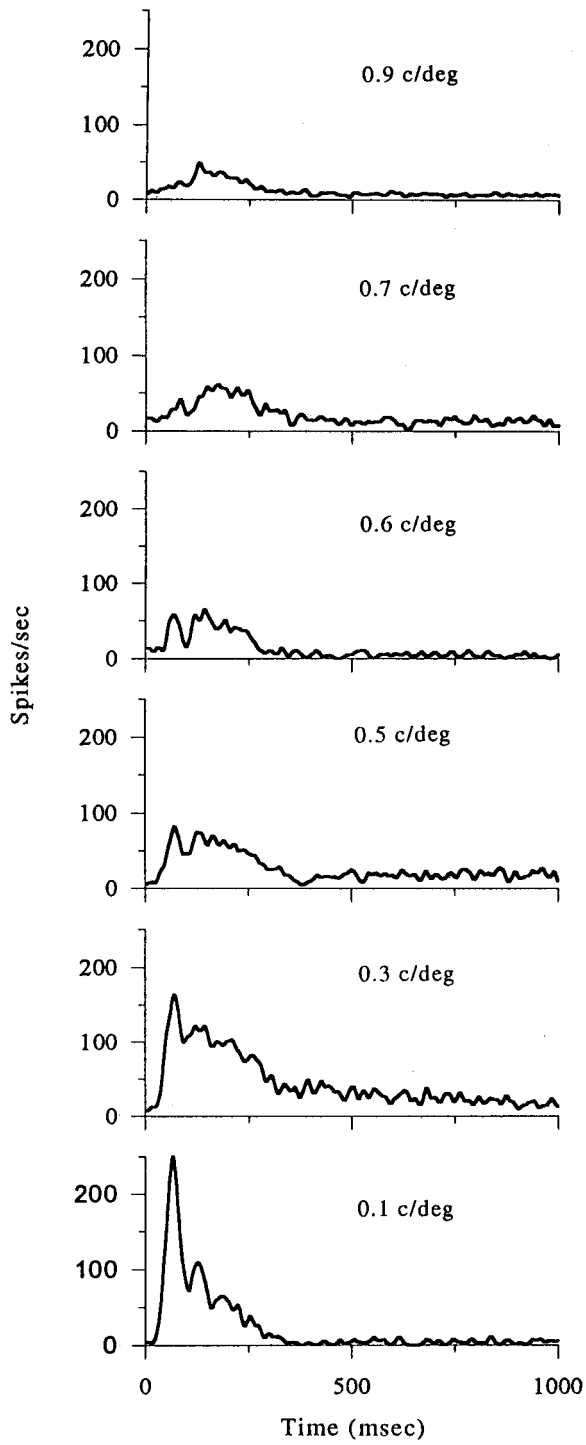

FIGURE 2. Positive step responses of an off center Y-cell at a series of spatial frequencies. Contrast was 19% for all spatial frequencies.

by computing the r^2 statistic. Isolated phase-dependent and phase-invariant profiles were compared with the overall response profiles to see if there was any temporal correspondence between the isolated profiles and the early and late peaks.

In the subtraction analysis, we first obtained an empirical estimate of the phase-invariant profile, by averaging responses from both half-cycles of the histogram collected at 0 deg of spatial phase. To estimate the phase-dependent portion of the response at each histogram, we subtracted our averaged estimate of the phase-invariant profile from each of the positive step response profiles. This also had the effect of removing DC firing levels from the estimate of the phase-dependent component of the response. Isolated phase-dependent and phase-invariant components were then compared to the early and late peaks of the overall responses. Phase-dependent response components, isolated by the subtraction method, were fitted to a widely accepted model of linear retinal ganglion cell dynamics, originally developed by Shapley and Victor (1981), who showed that it gives good fits to the linear responses of ganglion cells to frequency domain stimuli. The model consists of a transduction stage with a gain, A, followed by a cascade

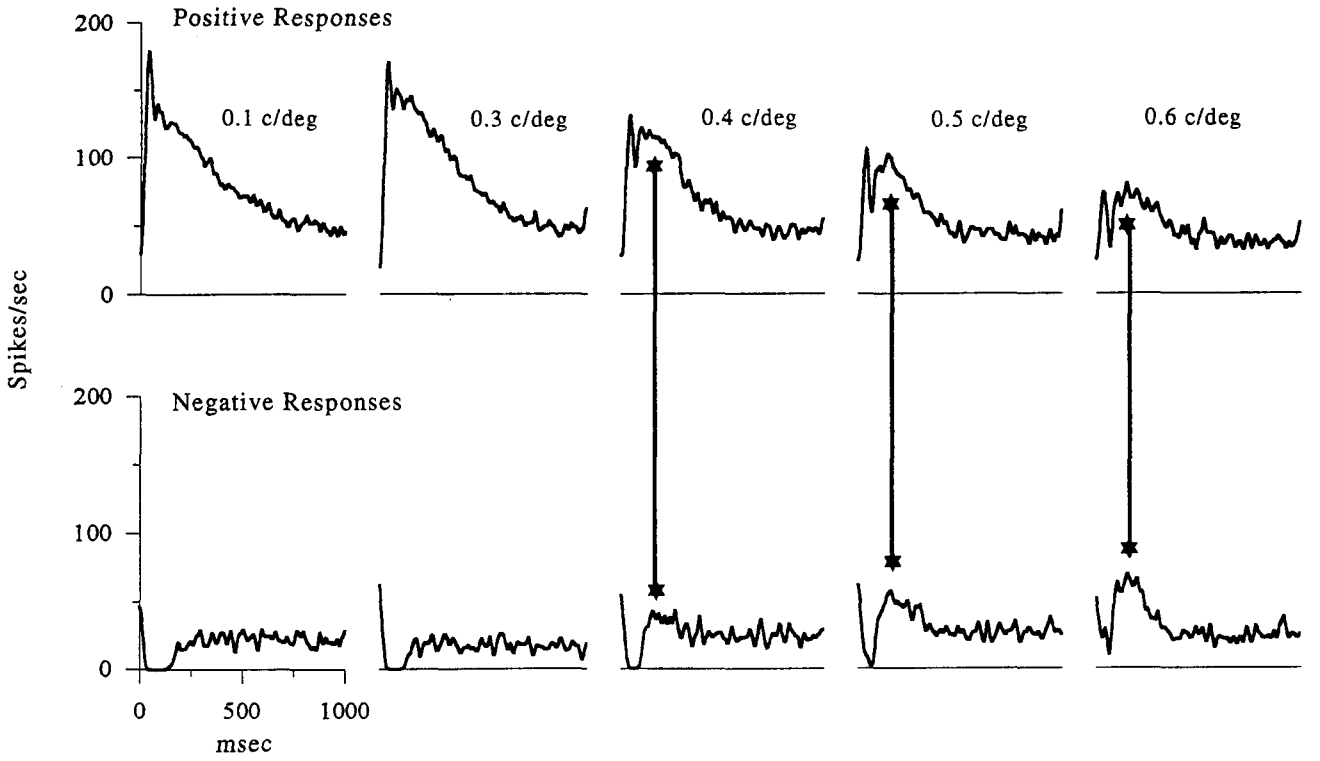

FIGURE 3. Positive and negative step responses of an off center Y-cell at a series of spatial frequencies. For each spatial frequency, the positive response is shown above, and the negative response below, with the onset of the positive and negative half-cycles aligned vertically. Contrast was 37% for all spatial frequencies. The thick vertical lines in the histograms for the three highest spatial frequencies indicate the temporal alignment of the late peaks in positive and negative responses. The duration of each histogram is 1 sec.

of low-pass filters, which is then followed by a single high-pass filter consisting of a low pass filter configured in a negative feedback loop with a gain of k. The transfer function of each stage of the low-pass filter is given by:

$$H_L(f) = \left(\frac{1}{1 + 2\pi i f T_L}\right)^{N_L}$$

while that of the high pass filter is

$$H_H(f) = \left(\frac{1}{1 + k/(1 + 2\pi i f T_H)}\right)$$

where f is frequency, T_L is the time-constant associated with each of the low-pass stages, N_L is the number of low-pass stages, T_H is the time-constant of the filter in the high-pass negative feedback loop, and k is the strength of the feedback. Thus, there were five free parameters in the model: the number of low-pass filters (N_L); the transducer gain (A); the low-pass time constant (T_L); the strength of the feedback (k); and the time-constant in the feedback loop (T_H). For each set of parameters tested, the frequency domain model was inverse transformed into the time domain and compared to the derived phase-dependent profiles. This procedure was repeated iteratively, using the Nelder–Mead algorithm mentioned above, until a minimum sum-of-squared error term was obtained. Two separate strategies were used for simultaneously fitting the profiles at different spatial phases. In one strategy, fits to all of the linear profiles in a given series were forced to share all parameters except for the transducer gain, which was constrained to remain within certain limits of the sine of the spatial phase of the stimulus used for each profile in the series. In a second strategy, all five parameters were allowed to vary freely.

RESULTS

Observations were made on a total of 35 ganglion cells. Representative step responses from three cells are shown in Fig. 1. Late peaks were rarely observed in on center X-cells, although they were occasionally seen in off center X-cells. On the other hand, late peaks were almost always evident in both on and off center Y-cell responses, although they sometimes were not fully separated from the early peak [Fig. 1(C)]. The latencies of the early and late peaks in Fig. 1(B) were *c.* 60 and 155 msec, respectively. These values can vary somewhat, but in general the two peaks differed in latency by 80–100 msec.

Dependence on spatial frequency

In order to evaluate the spatial frequency dependence of the two components, we measured step responses at a range of spatial frequencies in 15 cells. For each cell, responsivity was first assessed at a range of spatial frequencies, as described in Methods, in order to allow us to estimate the spatial resolution of the center and

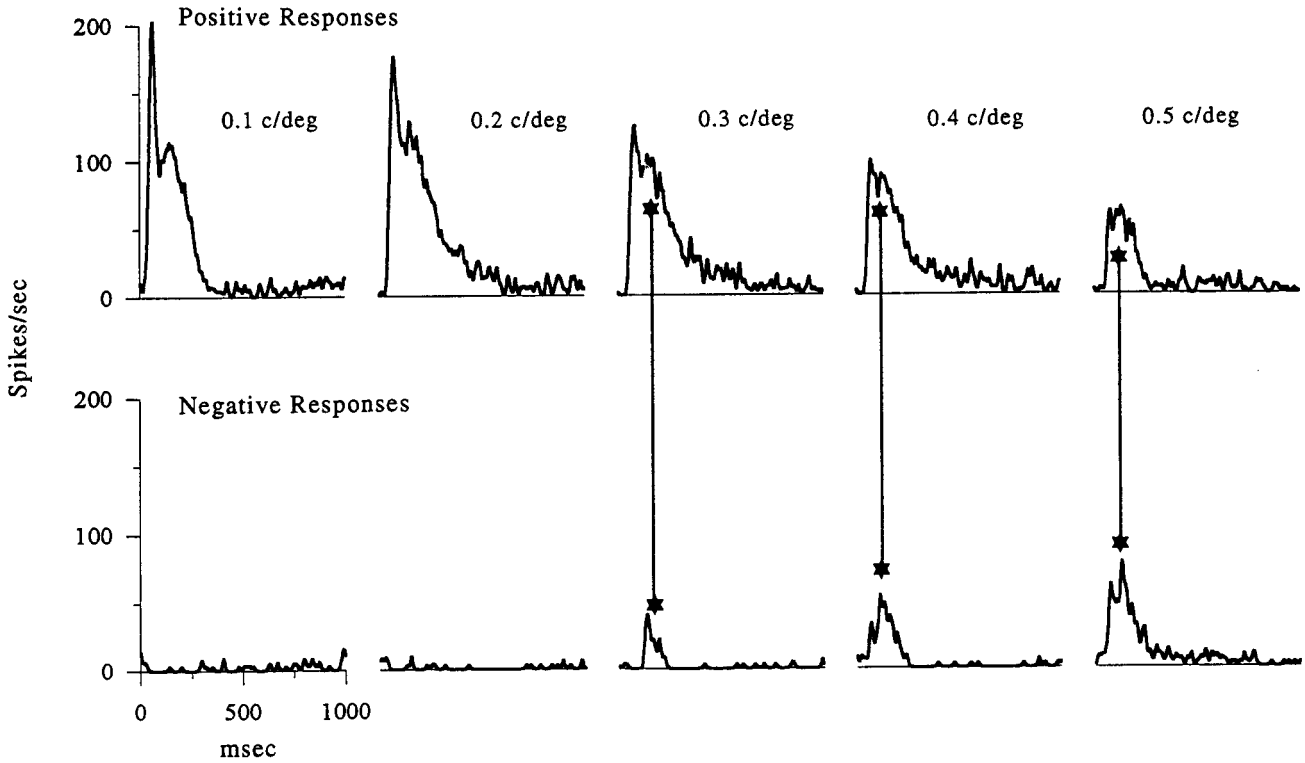

FIGURE 4. Positive and negative step responses of an on center Y-cell at a series of spatial frequencies. Conventions as in Fig. 3. Contrast was 37% at spatial frequencies of 0.1, 0.2, and 0.3 c/deg, and 68% at 0.4 and 0.5 c/deg. The duration of each histogram is 1 sec.

surround mechanisms. Step responses were then measured across a range of spatial frequencies that encompassed the spatial cutoff frequency of the surround, which we assumed to be near the peak of the spatial responsivity

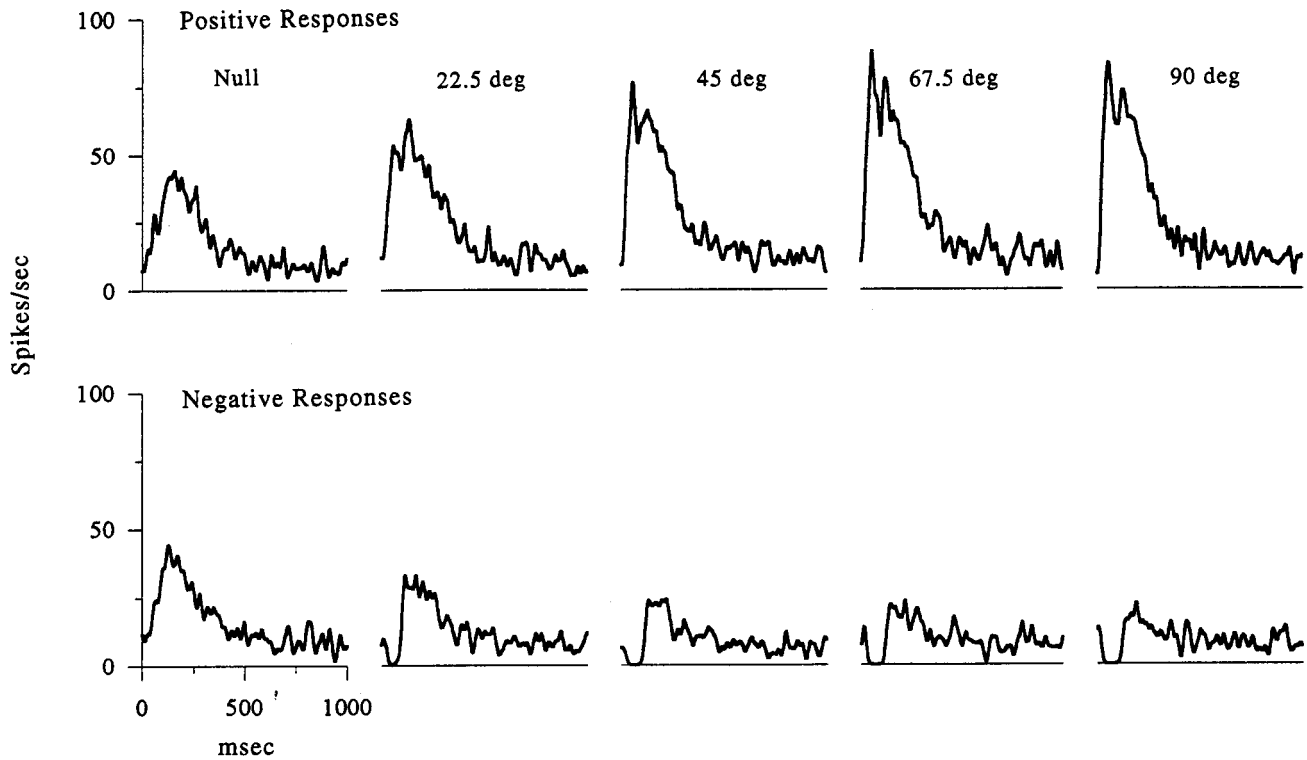

FIGURE 5. Positive and negative step responses of an off center Y-cell at a series of spatial phases. All measurements were made at a spatial frequency of 0.2 c/deg, which was the peak of the spatial responsivity function for this cell, and at a contrast of 25%. The duration of each histogram is one second.

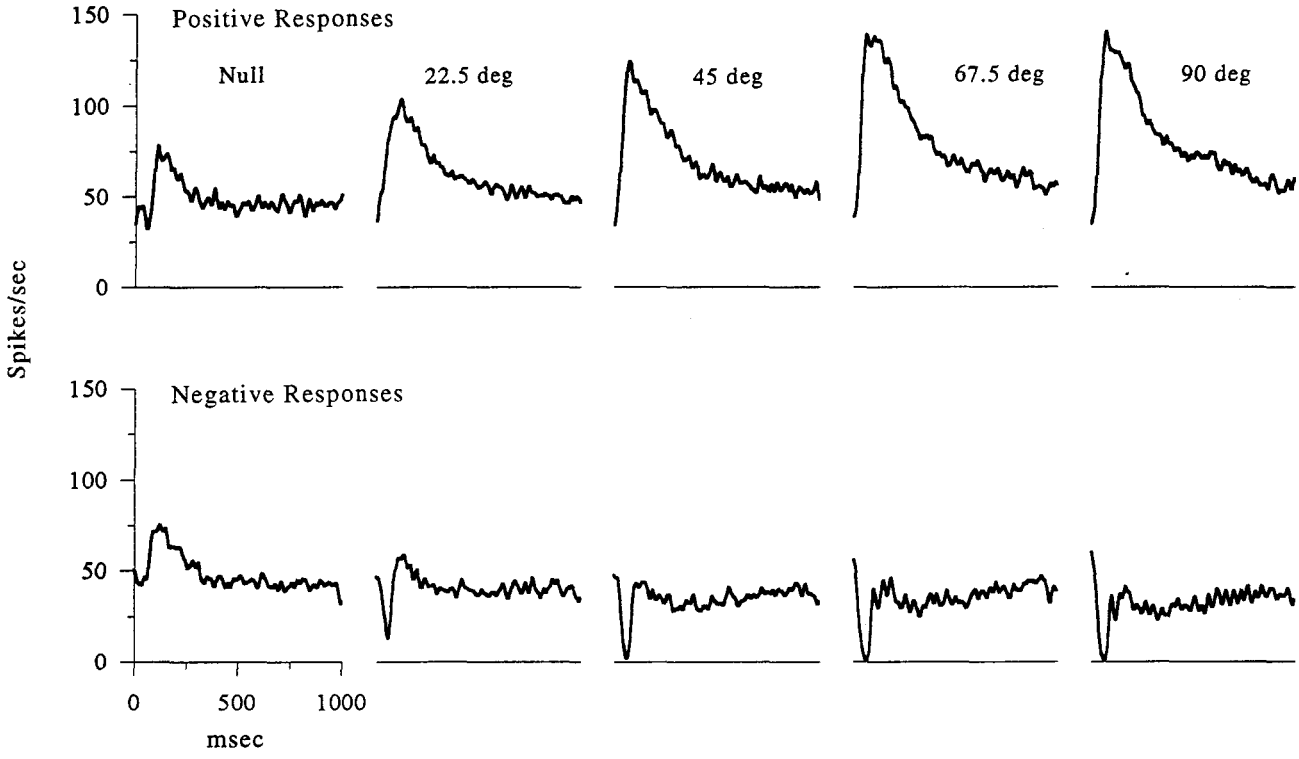

FIGURE 6. Positive and negative step responses of an on center Y-cell at a series of spatial phases. All measurements were made at a spatial frequency of 0.4 c/deg, which was above the peak of the spatial responsivity function (0.25 c/deg) for this cell, and at a contrast of 45%. The duration of each histogram is 1 sec.

function. The results obtained for one off center Y-cell are shown in Fig. 2. These histograms contain a number of interesting features. First, the early and late peaks show different patterns of dependence on spatial frequency; the early peak is largest at 0.1 c/deg and is virtually absent at 0.9 c/deg, while the late peak appears to be largest at about 0.5–0.6 c/deg, and is still obvious at 0.9 c/deg, suggesting that the mechanism underlying the late peak has a higher spatial resolution than that producing the early peak.

The contrast responsivity function for this cell was maximal at about 0.2 c/deg, and the best fitting DOG model indicated a spatial cutoff frequency for the surround of about 0.3 c/deg. Since both peaks in the step responses are clearly present at spatial frequencies up to 0.7 c/deg, neither could have been produced by the surround. This was a very consistent finding in all on and off center Y-cells examined in this way, and similar results were also obtained in a small number of off center X-cells.

These phenomena are readily apparent in positive step responses. However, negative step responses, i.e. the response to the half of the stimulus cycle that produced an initial decrease in firing rate, also contained useful information about the nature of the mechanisms underlying the two peaks. This is illustrated, for an off center Y-cell, in Fig. 3. The positive step response shows a pattern of spatial frequency dependence similar to that seen in Fig. 2, except that the maximum amplitude of the early peak is about 0.2 c/deg. All of the negative step responses begin with an initial decrease in firing rate, often reaching zero spikes/sec. At the three highest spatial frequencies tested, however, as the amplitude of the early peak is declining, a later, positive peak can be seen with approximately the same latency and time course as the late peak in the positive responses. A second example of this, for an on center Y-cell, is shown in Fig. 4. The spontaneous activity level of this cell was very low, so the features of the negative step responses can only be discerned at the higher spatial frequencies, but the temporal correspondence between the late peaks in the positive and negative responses is still evident. The latency and shape of the late peaks in positive and negative profiles suggests that they may be produced by a rectifying mechanism.

Dependence on spatial phase

We next evaluated the spatial phase dependence of the two components by examining both positive and negative step responses at a series of spatial phases (0, 22.5, 45.0, 67.5, 90.0 deg) in 13 Y-cells as well as two X-cells. Results from one off center Y-cell are shown in Fig. 5. The format of this figure is the same as in Figs 3 and 4, except that the independent parameter is now spatial phase. At a spatial phase of zero, the early peak is absent in both the positive or negative responses, and the responses to both cycles of the contrast reversal are essentially identical. This is the familiar frequency doubling behavior that has been previously reported in Y-cells and attributed to input from rectifying subunits

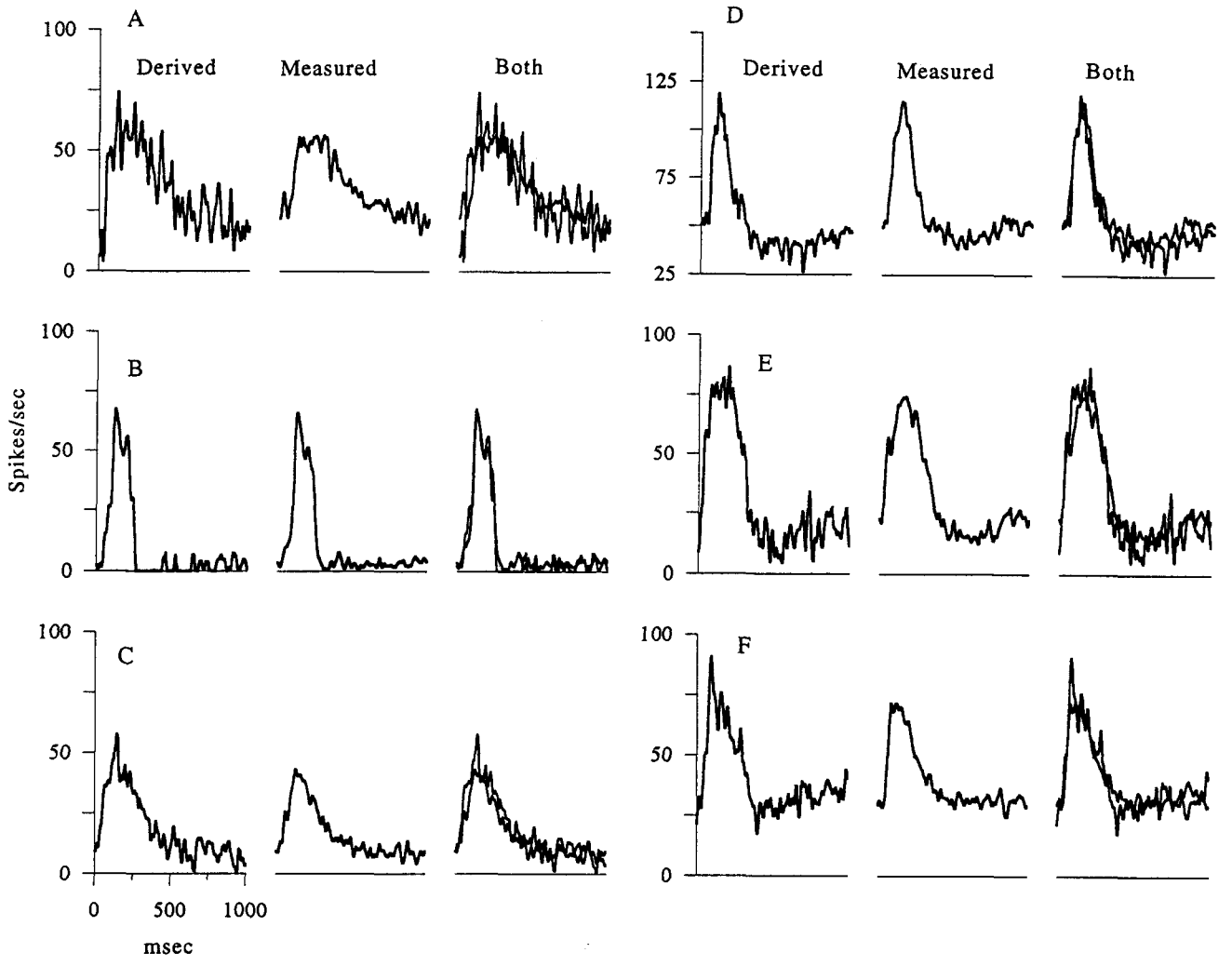

FIGURE 7. Comparisons of the phase-invariant profile derived by decomposition of the responses at nonzero spatial phases with the measured response at zero spatial phase for three off center Y-cells (A,B,C) and three on center Y-cells (D,E,F). For each cell, three histograms are shown: the profile derived from the decomposition (left), the measured response at zero spatial phase (middle), and the derived and measured profiles superimposed (right). The duration of each histogram is 1 sec.

(Hochstein & Shapley, 1976a,b; Victor, 1988). In the positive step responses, both early and late peaks are evident at all nonzero spatial phases, and the amplitude of the early peak is clearly phase dependent. In the negative step responses, the late peak appears to become smaller and shifted downwards as spatial phase increased due to the inhibition produced by the early component. A second phase series, from an on center Y-cell, is shown in Fig. 6. The overall pattern of phase dependence is the same, but in this case the higher maintained firing rate of the cell allowed the details of the negative response to be seen more clearly.

Decomposition analysis

The phase data just presented provide a qualitative indication that size of the early peak in the step response is dependent on spatial phase while that of the late peak is independent of spatial phase. We next examined this possibility more rigorously using the decomposition analysis described in Methods to separate phase-dependent and phase-independent components of the response. Profiles at all nonzero spatial phases (22.5, 45.0, 67.5 and 90.0) provided a basis for the decomposition analysis. The analysis yielded a single phase-dependent profile, which was then scaled by the sine of each of these spatial phases to obtain an estimate of the phase-dependent response component at each phase, as well as a phase-invariant profile which served as an estimate of the phase-invariant response component at all spatial phases.

As an internal check of the validity of the decomposition, we first compared the phase-invariant profile derived from decomposition of responses at nonzero spatial phases with the actual responses measured at the zero-phase position. According to our assumptions, these should be identical, and as can be seen in Fig. 7, the correspondence was quite good. Using the r^2 statistic to evaluate the correspondence between the derived and measured zero-phase profiles over 23 separate sets of phase series data, we found that the median value of r^2 was over 0.90.

A direct comparison of the phase-dependent and phase-independent components derived from the decomposition

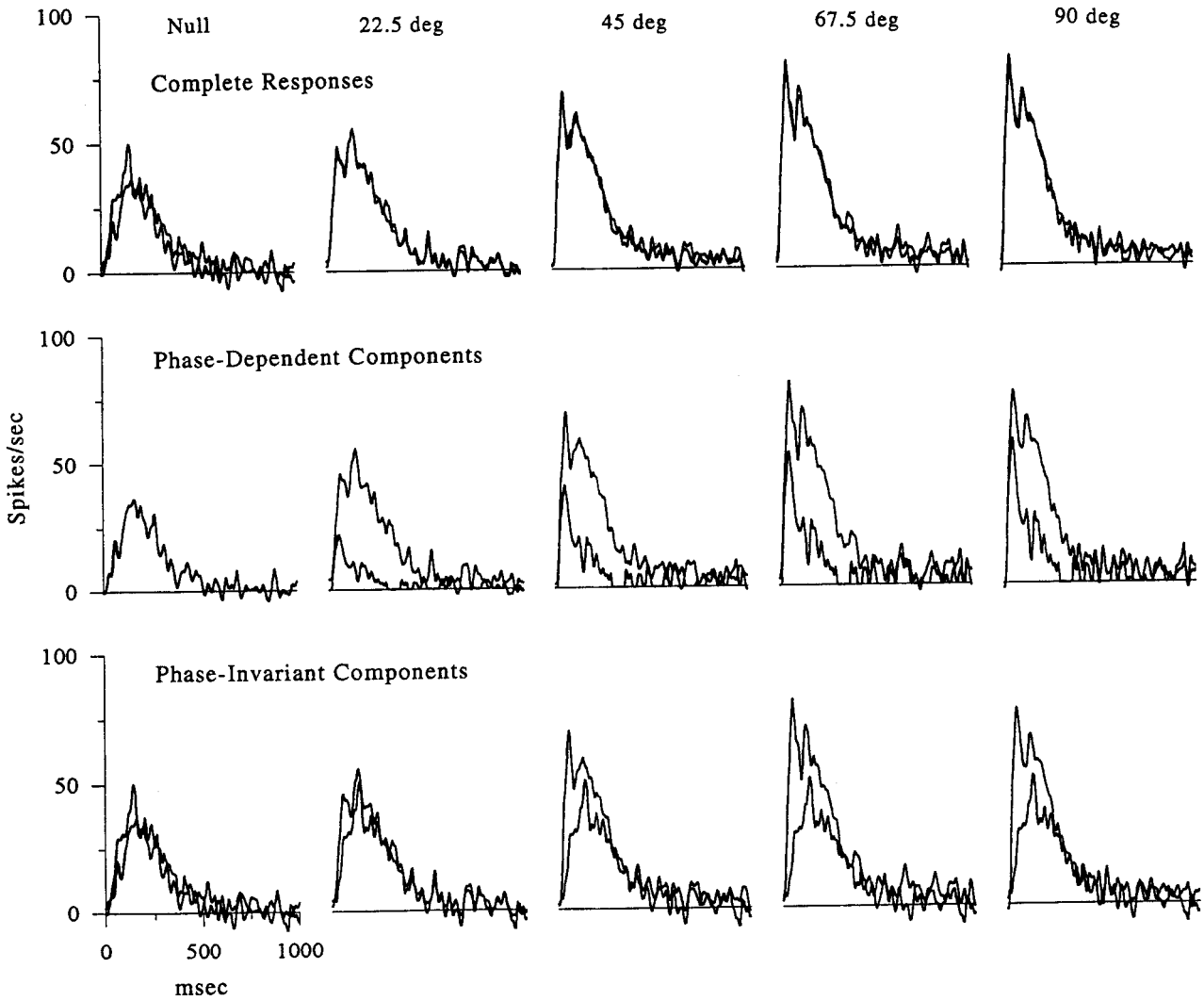

FIGURE 8. Comparison of phase-dependent and phase-independent response components derived from the decomposition analysis with the measured responses at all spatial phases. The middle row of histograms shows the measured response at each spatial phase superimposed on the derived phase-dependent component, and the bottom row of histograms shows the measured response superimposed on the derived phase-independent component. The top row of histograms shows the sum of the two derived components superimposed on the measured responses. The duration of each histogram is 1 sec. In this figure, the DC components have been removed from the response profiles.

analysis with the measured responses at each spatial phase is shown in Fig. 8 for an on center Y-cell. It is clear that the timing and overall shape of the derived phase-dependent and phase-independent components match quite well those of the early and late peaks, respectively, at all spatial phases, and that the sum of the derived components is a very good approximation of the measured responses. The combined results presented in Figs 7 and 8 suggest that the shape of the phase-dependent response at any spatial phase can also be seen in isolation by subtracting the response at zero spatial phase from the overall response at any nonzero spatial phase, and this is illustrated for an on Y-cell in Fig. 9. Here also, it is clear that the estimate of the phase-dependent component produced by the subtraction had a shape and time course very similar to that of the early peak in the response at each spatial phase, and that the timing of the zero phase response matched that of the late peaks at each spatial phase.

Fits to the linear cascade model

Our assumption in using the decomposition and subtraction procedures just described was that the early response component was produced by the spatially linear center mechanism, and it was therefore of interest to see how well the derived phase-dependent component could be described by a linear model of retinal ganglion cell dynamics (Shapley & Victor, 1981; Victor, 1987). As described in the Methods, two strategies were used to fit this linear cascade model to linear profiles derived by subtraction of the zero spatial phase response from responses at other spatial phases. In the first, fits to all of the linear profiles in a given series were forced to share all parameters, except for a scaling factor that varied with spatial phase, i.e., the fitted profiles at each spatial phase

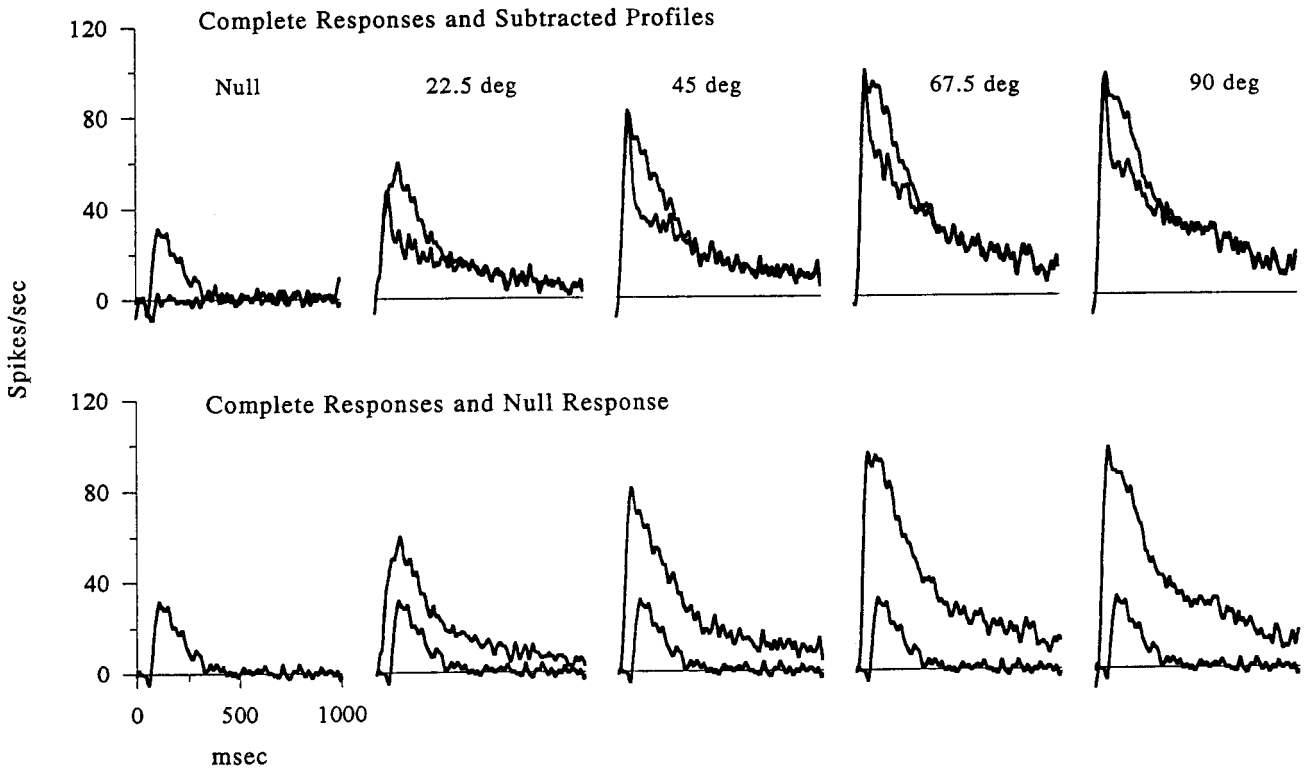

FIGURE 9. Isolation of phase-dependent response component by subtraction of response at zero spatial phase from responses at nonzero spatial phases for an off center Y-cell. The top histograms show the measured response at each spatial phase superimposed on the phase-dependent component produced by the subtraction procedure, and the bottom histograms show the measured response superimposed on the response at zero spatial phase. The duration of each histogram is 1 sec. In this figure, the DC components have been removed from the response profiles.

were identical in shape, but their sizes were set by separate scaling factors. In the second strategy, all parameters were allowed to vary freely for all spatial phases. The two procedures yielded essentially identical results, so only those from fits with shared parameters are illustrated. Representative examples from three on center and three off center Y-cells are shown in Fig. 10. The subjective quality of these fits varies from good to excellent. When fits were less than excellent, it was generally because the fit failed to perfectly reflect the initial rise in firing rate. Occasionally, some remnant of the late peak appeared to be present in the subtracted profiles, which diminished the quality of the fits.

Goodness-of-fit statistics were also tabulated for all fits. For spatial phases of 45.0, 67.5, and 90.0 deg, the median value of r^2 was 0.85, and at 22.5 deg, the median value was 0.69. The lower value at this spatial phase presumably reflects the lower signal-to-noise level. The r^2 values for fits where all parameters were free to vary were generally only slightly better. The values of the best

TABLE 1. Fitted parameters for the linear cascade model

Panel	Cell	SF	CON	N_L	A	T_L	k	T_H	$N_L T_L$	k/T_H
A	Off-Y	0.2	0.25	7.999	69.872	3.881	10.450	1.310	31.04	7.98
B	Off-X	0.5	0.20	12.000	129.471	2.012	1.837	.198	24.15	9.27
C	Off-Y	0.5	0.45	18.854	60.516	2.204	7.002	1.749	41.55	4.00
D	On-Y	0.5	0.45	11.533	151.680	2.796	4.385	1.750	32.25	2.51
E	On-Y	0.2	0.45	6.400	172.372	2.980	10.200	1.020	19.07	10.00
F	On-Y	0.4	0.25	9.830	100.751	3.395	3.320	1.133	33.37	2.93

Parameters of the best fitting linear cascade model for the fits shown in Fig. 10. The first four columns identify the corresponding panel in Fig. 10, the receptive field type, the spatial frequency (SF) and the contrast (CON) used. Remaining columns give the five parameters of the best fitting model, as well as the ratio k/T_H and the product $N_L T_L$. Dimensions of the parameters are as follows: T_L (time-constant in the feedback loop) is specified in msec; T_H (low-pass time-constant) is specified in sec; A (transducer gain) is given in spikes/sec; other parameters are dimensionless. The curve fitting program allowed N_L (the number of low-pass filters) to assume noninteger values, as shown here, by using a linear interpolation procedure. Fits were obtained using the parameters-shared strategy with T_H constrained to be no greater than 1.75 sec and with N_L constrained to be between 6 and 28 filters. With these constraints, the values that we obtained are similar to values obtained by Shapley and Victor (1981). k, strength of the feedbacks.

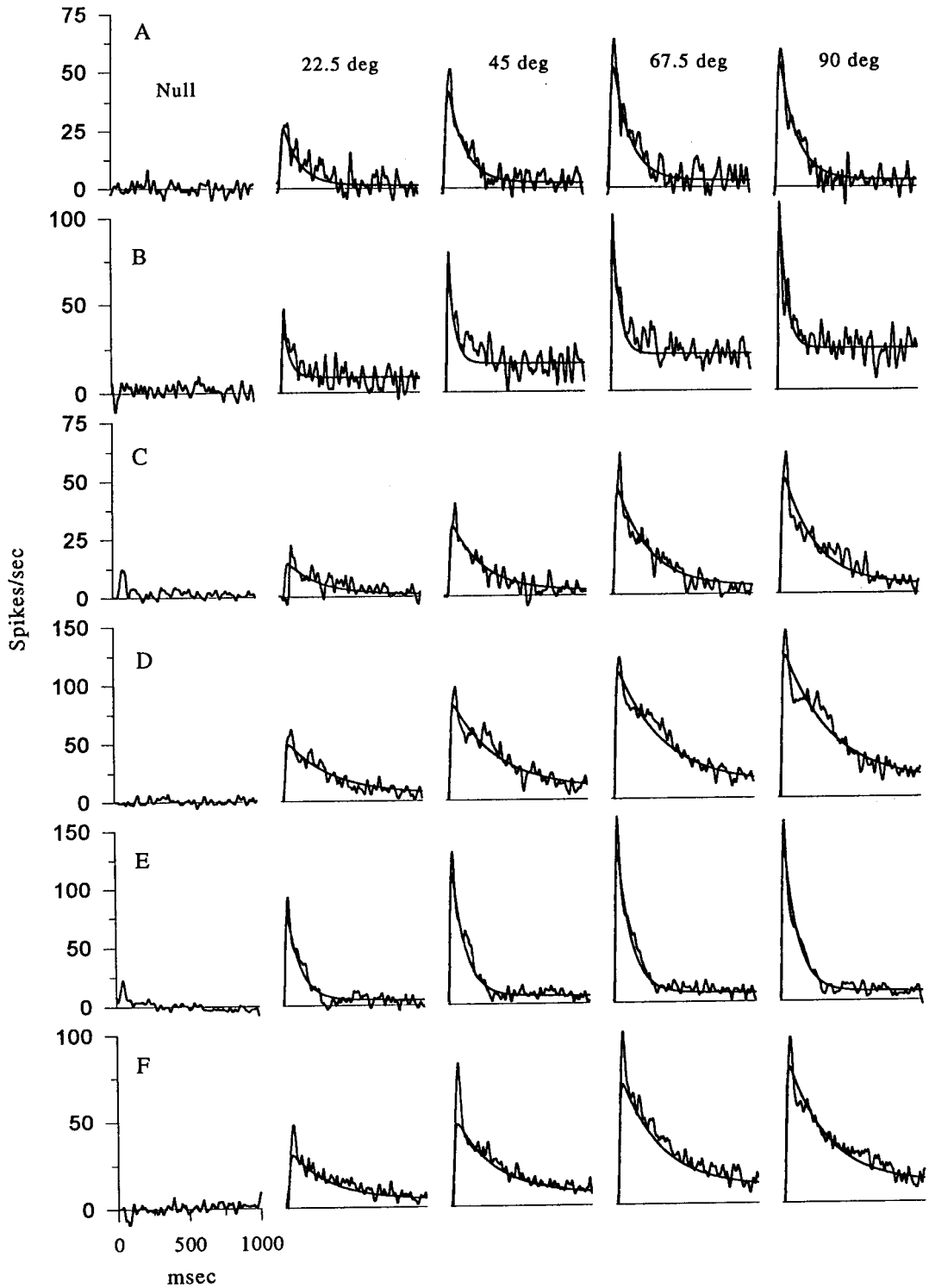

FIGURE 10. Fits of the linear cascade model (smooth lines) to estimated linear response components at different spatial phases for three off center (A,B,C) and three on center (D,E,F) Y-cells. The linear responses were estimated by subtraction of the zero-phase responses from the overall responses at each of the other spatial phases. The duration of each histogram is 1 sec.

fitting parameters for the cells shown in Fig. 10 are shown in Table 1. The values are generally similar to the values reported by Shapley and Victor (1981).

Effects of reducing mean luminance

Since our stimulus illumination was at a mesopic level, we were interested to see whether or not the shape of the step responses was dependent on the presence of both rod and cone signals. To do this, we first measured step responses for an off center Y-cell at the usual mean luminance of the display, which is mesopic for cats. Then a 2 log unit neutral density filter was placed in front of the

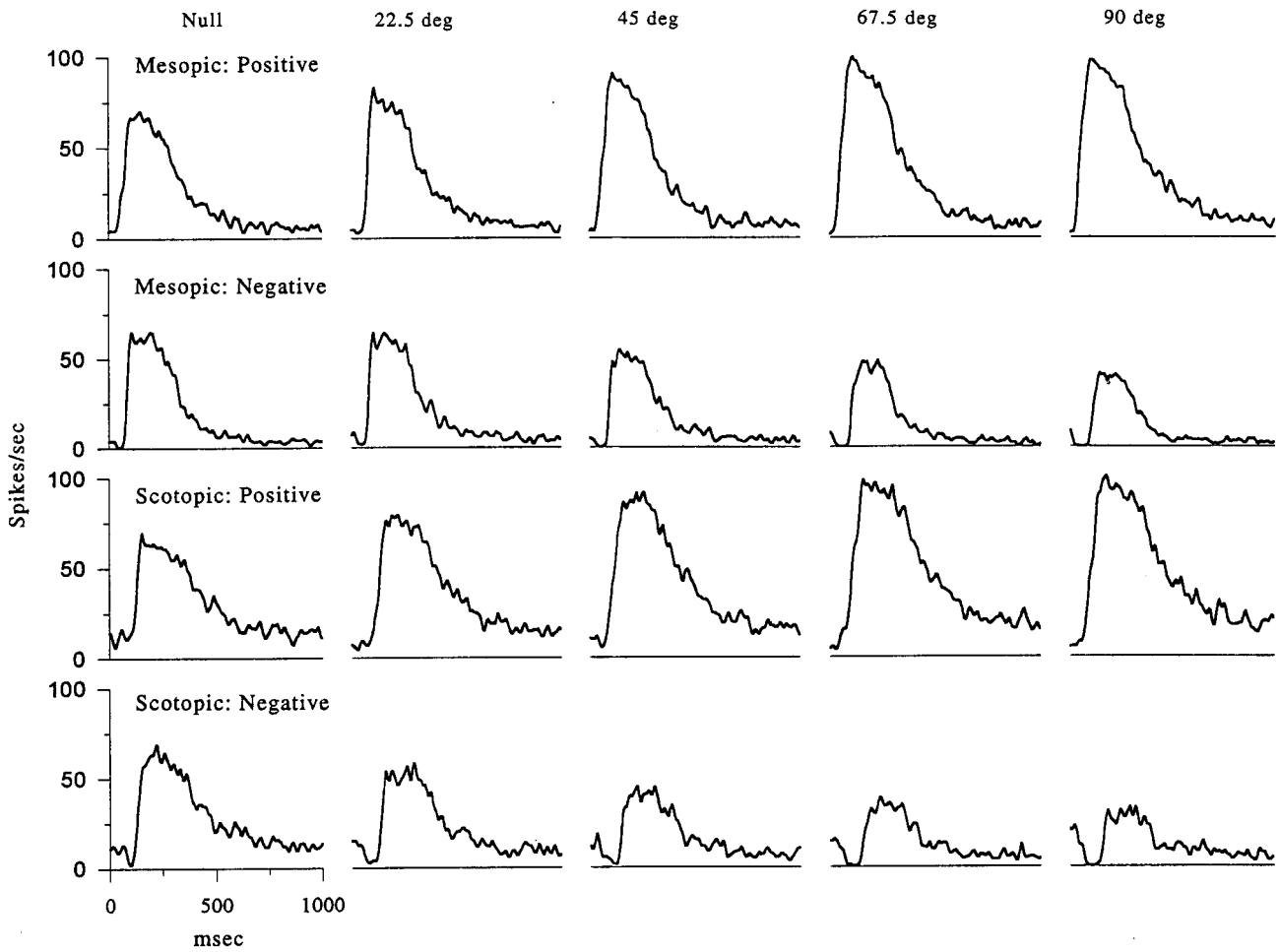

FIGURE 11. Positive and negative step responses of an off center Y-cell at the normal, mesopic screen luminance of 3 cd/m^2 (top two rows), and with luminance reduced to scotopic levels by a 2 log unit neutral density filter (bottom two rows). Comparison of positive and negative responses indicates that early (nonrectified) and late (rectified) peaks are both clearly evident at the reduced luminance level, although both are at distinctly longer latencies. The stimulus was an alternating grating of 0.5 c/deg and a contrast of 40%. Responses are shown at spatial phases of 0, 22.5, 45, 67.5, and 90 deg. The duration of each histogram is 1 sec.

eye, reducing the image brightness to scotopic levels, and the cell was allowed to adapt to the lower luminance for 30 min, after which the step responses were measured again. The results are shown in Fig. 11. Both early and late peaks are still present at the lower mean luminance, indicating that cone signals are not necessary for either of them.

DISCUSSION

The major findings of this study are:

(i) for cat retinal Y-cells excitatory step responses elicited by contrast reversal of a stationary sine wave grating contain two distinct peaks;
(ii) both peaks are present at spatial frequencies that are above the resolution of the receptive field surround;
(iii) the early peak is produced by a linear mechanism, but the late peak is produced by a rectifying mechanism;
(iv) the amplitude of the early peak shows an approximately sinusoidal dependence on the spatial phase of the grating, but the amplitude of the late peak is independent of spatial phase.

Similar results were seen in some off center X-cells, but these were not investigated as extensively. Taken together, these results suggest that the early peak in such step responses is produced by the spatially linear center mechanism, while the late peak is the result of an excitatory input from a spatially nonlinear mechanism with properties resembling those of the nonlinear subunits described by Hochstein and Shapley (1976a, b). These results further suggest that it is not necessary to invoke a delayed inhibitory mechanism to explain the shape of the step response (Saito *et al.*, 1971; DeMonasterio, 1978; Richter & Ullman, 1982), since the two peaks of the step response appear to be fully accounted for by the combination of two excitatory signals converging on the ganglion cell, each associated with a distinct component of the ganglion cell's receptive field. These results provide clear support for the model of Y-cell receptive fields first proposed by Hochstein and Shapley (1976a, b), and are also consistent with previous work by

Victor (1988), who modeled the frequency-domain responses of the nonlinear response mechanism in cat Y-cells, and found that the integration times of the nonlinear response mechanisms, extracted from his model, were longer than the integration times of the linear response component.

Although our conclusions strictly apply only to cat retinal ganglion cells, there are a number of notable similarities between our data and those presented by DeMonasterio (1978) from primate retina. In that paper, step responses with two peaks were only observed in cells exhibiting nonlinear spatial summation, which DeMonasterio referred to as Y-like or type IV cells (more recent classifications include Y-like cells as a subset of the group designated as M-cells). DeMonasterio further noted that the two peaks persisted in the presence of scotopic backgrounds, and that the underlying mechanism appeared to involve some degree of rectification, thereby resembling the nonlinear mechanism seen in cat Y-cells. Thus, although it remains to be directly demonstrated, it is possible that the shape of step responses in some primate M cells can also be explained by a combination of linear and nonlinear excitatory inputs with different time courses.

Alternative mechanisms

Our results also appear to exclude at least two other possible explanations for the presence of two peaks in ganglion cell step responses:

(i) the possibility that the appearance of the step response reflects known differences in timing between center and surround mechanisms (Winters & Hamasaki, 1976; Derrington & Lennie, 1982; Enroth-Cugell *et al.*, 1983; Dawis *et al.*, 1984; Frishman *et al.*, 1987);
(ii) the possibility that the two components are due to differences in timing between rod and cone signals reaching the ganglion cells in mesopic conditions.

Earlier examples of two-peaked step responses in both cat (Winters & Walters, 1970; Saito *et al.*, 1971) and monkey (DeMonasterio, 1978) involved stimuli that activated both center and surround mechanisms, and it is possible under such conditions that latency differences between center and surround mechanisms could produce the transient dip observed in the step response. In our experiments, however, we routinely used gratings that were above the resolution of the surround mechanism, and the basic features of the step response remained intact. Moreover, center–surround latency differences have been estimated to be much smaller than the latency of the dip that separates the two peaks of the step responses (Dawis *et al.*, 1984; Frishman *et al.*, 1987), and it is not likely that this feature of the response depends on surround activation.

Rod and cone signals are both clearly present at the mesopic illumination levels used here, and it is clear, both from earlier work (Troy *et al.*, 1993) and from Fig. 11 that rod mediated responses in ganglion cells are slower than cone mediated responses. However, rod and cone inputs to ganglion cells are more or less spatially coextensive, and there is no reason to suspect that one of these signals would be dependent on spatial phase while the other was phase independent. Furthermore, both components of the step response were clearly evident at scotopic illumination levels, where cone signals were absent. Thus, the presence of two peaks in ganglion cell step responses does not appear to be critically dependent on activation of both rod and cone inputs.

It is also noteworthy, in the context of alternative explanations, that the appearance of two peaks in the step responses is not an artifact of any particular anesthetic. Winters and Walters (1970) used unanesthetized, decerebrate cats, and recorded step response from retinal ganglion cells that are remarkably similar to ours (compare their Fig. 6 to our Fig. 1).

Validity of the decomposition analysis

The strongest evidence supporting the linear/nonlinear hypothesis was obtained by numerical decomposition of the step responses at different spatial phases into phase-dependent and phase-independent components. There were four basic assumptions underlying this method:

(i) a phase-invariant mechanism contributes to the response;
(ii) a mechanism that is sinusoidally-dependent on spatial phase contributes to the response;
(iii) the outputs of these two mechanisms combine additively; and
(iv) these two mechanisms are the only mechanisms that contribute to the response.

If any of these assumptions are invalid, then the decomposition method is also invalid. Nevertheless, we are confident in the validity of the decomposition method because it was able to predict the response at a spatial phase of 0 deg with considerable accuracy (Figs 7 and 8). As a further test of the method, however, we performed the analysis on phase series data from an on center X-cell in which the responses to the contrast reversals at 0 spatial phase were essentially flat, and in this case, the decomposition procedure also produced a phase-independent component that was flat. The fact that a well accepted linear cascade model of retinal ganglion cell dynamics gave good or excellent fits to our isolated linear profiles, even though the model was developed for frequency domain data and our data were in the time domain, also supports the validity of our analysis.

Implications for modeling step responses

Step responses can be used to evaluate models of retinal ganglion cell dynamics based on frequency domain data. When applied to cells that do not show significant second order nonlinearities (e.g. Victor, 1987) this is not problematic. Our results show that for Y-cells, however, both linear and nonlinear receptive field mechanisms contribute to their step responses, rendering them unsuitable for testing linear models, unless the

nonlinear component is removed. The decomposition analysis further suggests that a simple way to do this, at least in cases where the spatial profile of the stimulus used is in the form of a sinusoidal grating, is to measure step responses at zero spatial phase of the grating, and subtract this response from the responses obtained at other spatial phases. This produces a response profile that can be well fitted to linear models of temporal dynamics. If the spatial configuration of the stimulus is something other than a grating, e.g. a circular spot or a rectangle, an alternative method would be to measure the response to both increments and decrements of equal magnitude from a common luminance value and subtract the negative response profile from the positive response profile. In general, this manipulation will remove second order nonlinearities (McLean & Palmer, 1989), and is equally appropriate for producing a linear temporal response profile.

REFERENCES

Cleland, B. G., Dubin, M. & Levick, W. R. (1971). Sustained and transient cells in the cat's retina and lateral geniculate nucleus. *Journal of Physiology, London, 217*, 473–496.

Cox, J. F. & Rowe, M. H. (1993). Nonlinear contributions to the step responses of cat retinal ganglion cells. *Society for Neuroscience, Abstracts, 19*, 1417.

Dawis, S. M., Shapley, R. M., Kaplan, E. & Tranchina, D. (1984). The receptive field organization of x cells in the cat: Spatiotemporal coupling and asymmetry. *Vision Research, 24*, 549–564.

DeMonasterio, F. M. (1978). Center and surround mechanisms of opponent-color X and Y ganglion cells of retina of macaques. *Journal of Neurophysiology, 41*, 1418–1434.

Derrington, A. M. & Lennie, P. (1982). The influence of temporal frequency and adaptation level on receptive field organization of retinal ganglion cells in cat. *Journal of Physiology, London, 333*, 343–366.

Enroth-Cugell, C. & Robson, J. G. (1966). The contrast sensitivity of retinal ganglion cells of the cat. *Journal of Physiology, London, 187*, 517–552.

Enroth-Cugell, C., Robson, J. G., Schweitzer-Tong, D. E. & Watson, A. B. (1983). Spatio-temporal interactions in cat retinal ganglion cells showing linear spatial summation. *Journal of Physiology, London, 341*, 279–307.

Enroth-Cugell, C. & Shapley, R. M. (1973). Adaptation and dynamics of cat retinal ganglion cells. *Journal of Physiology, London, 233*, 271–309.

Frishman, L. J., Freeman, A. W., Troy, J. B., Schweitzer-Tong, D. E. & Enroth-Cugell, C. (1987). Spatiotemporal frequency responses of cat retinal ganglion cells. *Journal of General Physiology, 89*, 599–628.

Hammond, P. (1975). Receptive field mechanisms of sustained and transient retinal ganglion cells in the cat. *Experimental Brain Research, 23*, 113–128.

Hochstein, S. & Shapley, R. M. (1976a). Quantitative analysis of retinal ganglion cells. *Journal of Physiology, London, 262*, 237–264.

Hochstein, S. & Shapley, R. M. (1976b). Linear and nonlinear spatial subunits in Y cat retinal ganglion cells. *Journal of Physiology, London, 262*, 265–284.

Ikeda, H. & Wright, M. J. (1972). Receptive field organization of "sustained" and "transient" retinal ganglion cells which subserve different functional roles. *Journal of Physiology, London, 227*, 769–800.

Jakiela, H., Enroth-Cugell, C. & Shapley, R. M. (1976). Adaptation and dynamics in X-cells and Y-cells of the cat retina. *Experimental Brain Research, 24*, 335–342.

Linsenmeier, R. A., Frishman, L. J., Jakiela, H. G. & Enroth-Cugell, C. (1982). Receptive field properties of X and Y cells in the cat retina derived from contrast sensitivity measurements. *Vision Research, 22*, 1173–1183.

McLean, J. & Palmer, L. A. (1989). Contribution of linear spatiotemporal receptive field structure to velocity selectivity of simple cells in area 17 of cat. *Vision Research, 29*, 675–679.

Nelder, J. A. & Mead, R. (1965). A simplex method for function minimization. *Computer Journal, 7*, 308–313.

Pettigrew, J. D., Cooper, M. L. & Blasdel, G. G. (1979). Improved use of tapetal reflection for eye-position monitoring. *Investigative Ophthalmology and Visual Science, 18*, 490–495.

Richter, J. & Ullman, S. (1982). A model for the temporal organization of X- and Y-type receptive fields in the primate retina. *Biological Cybernetics, 43*, 127–145.

Rowe, M. H. & Stone, J. (1976). Conduction velocity groupings among cat retinal ganglion cell axons and their relationship to retinal topography. *Experimental Brain Research, 25*, 339–357.

Saito, H., Shimihara, T. & Fukada, Y. (1971). Phasic and tonic responses in the cat optic nerve fibers—stimulus–response relations. *Tohoku Journal of Experimental Medicine, 102*, 127–133.

Shapley, R. M. & Victor, J. D. (1981). How the contrast gain control modifies the frequency responses of cat retinal ganglion cells. *Journal of Physiology, London, 318*, 161–179.

Troy, J. B., Oh, J. K. & Enroth-Cugell, C. (1993). Effect of ambient illumination on the spatial properties of the center and surround of Y-cell receptive fields. *Visual Neuroscience, 10*, 753–764.

Victor, J. D. (1987). The dynamics of the cat retinal X-cell centre. *Journal of Physiology, London, 386*, 219–246.

Victor, J. D. (1988). The dynamics of the cat retinal Y cell subunit. *Journal of Physiology, London, 405*, 289–320.

Winters, R. W. & Hamasaki, D. I. (1976). Temporal characteristics of peripheral inhibition of sustained and transient ganglion cells in cat retina. *Vision Research, 16*, 37–45.

Winters, R. W. & Walters, J. (1970). Transient and steady state stimulus–response relationships for cat retinal ganglion cells. *Vision Research, 10*, 461–467.

Acknowledgements—This work was performed in partial fulfilment of the requirements for the PhD in Biological Sciences at Ohio University. The work was supported in part by a grant from the NEI (EY08038) and by funds from the Ohio University College of Osteopathic Medicine.